Original Article

Institution of MECHANICAL ENGINEERS

Journal of NANOENGINEERING AND NANOSYSTEMS

Proc IMechE Part N: J Nanoengineering and Nanosystems
226(1) 15–22

DOI: 10.1177/1740349912444511
pin.sagepub.com
SAGE

Developing microfluidics for rapid protoplasts collection and lysis from plant leaf

Min-Sheng Hung and Jia-Hao Chang

Abstract

This study develops polydimethylsiloxane microfluidics to enable real-time collection and lysis of *Phalaenopsis* protoplasts and to analyze and compare the protoplast collecting efficiency of a concave sieving array with that of a convex–concave sieving array. Each set of microfluidics comprises a main flow channel and a protoplast sieving array with collecting channels. The protoplasts were isolated from *Phalaenopsis* leaves by an enzymatic breakdown of the cell walls and collected in side channels through microsieves. Finally, 1% w/v sodium dodecyl sulfate solution was injected into lysed protoplasts, and the DNA segment of the lysed protoplasts was released into the solution. The results indicate that the concave sieving array at the U-bend of the main flow channel causes the protoplasts to flow back into the main flow channel from the collecting channels. Thus, the protoplast collecting efficiency of the concave sieving array was lower in this study. Regarding the number and arrangement of protoplast microsieves, the convex–concave sieving array substantially restricts protoplasts from flowing back into the main flow channel, thereby increasing the collecting efficiency. Finally, DNA is released from lysed protoplasts after the injection of a lysis solution. DNA flow can be focused into a single stream to contact the rectangular microstructures in microchannels.

Keywords

Sieving array, protoplast collection, protoplast lysis, polydimethylsiloxane microfluidics

Date received: 13 January 2012; accepted: 14 March 2012

Introduction

In recent years, the speed of technology used for decoding gene sequences has significantly improved. In addition to animal and plant DNA, the genomes of bacteria and even viruses have been successfully sequenced. However, because of varying operating conditions, the time required for sample analysis differs. Furthermore, the cost of analysis is high and the sample preprocessing procedures present complications. Therefore, a microfabricated real-time platform that can perform detections using a small sample and reagents must be developed to reduce costs and analysis time.

Numerous researchers and specialists have explored the application of microchips to biological samples (e.g. blood, tissue, cells, proteins and nucleic acids) for more efficient analysis. Thus, the objective of this study is to employ microfabrication technologies to construct a microanalysis system that uses a small analytical sample and a biochemical reagent to detect biological samples. The results can hopefully contribute to developing a micro total analysis system (μ-TAS),[1–3] shortening sample analysis time and reducing analysis costs.

The current biological or medical procedures used to analyze samples in common laboratories involving complex fluids with cells (e.g. blood) typically require preparative collection of cells or even molecules. Thus, cell collection presents a major obstacle in μ-TAS development.[3] The most straightforward method of cell separation in microfluidic systems is to use filtration sieves under laminar flow. These studies are used for cell separation based on the cell size and morphology.[4] For example, Kuo et al.[5] designed and used microfluidics to capture cancer cells by separating cells according to size. In this method, cell solution was passed through microchannels before the larger cancer cells were captured by the channels within the structure; then, the other substances flowed towards the waste outlet. If the

Department of Biomechatronic Engineering, National Chiayi University, Taiwan

Corresponding author:
Min-Sheng Hung, Department of Biomechatronic Engineering, National Chiayi University, Chiayi 600, Taiwan.
Email: mshung@mail.ncyu.edu.tw

cell size and morphology are similar, such as the live and dead cells, cell isolation becomes difficult.

Current cell separation techniques that employ microfluidics and non-inertial forces include dielectrophoretic force using cell size and dielectric properties to isolate cells;[6,7] optical force using a focused laser beam to trap cells;[8] and magnetic force using magnetic beads to label cells.[9] For example, Lien et al.[10] used magnetic forces to separate cells. In their study, air pressure was used to control the mixing and flow direction of the liquid before modified magnetic beads were added to the solution. Then cancer cells in the blood were captured using the antigen–antibody binding method. The integrated numerous separation methods can be used to separate mixtures of two or more cells based on the varied separation modes, resolution, efficiency and physiological effects.

Cell lysis is the first step in detecting substance (e.g. nucleic acid, proteins) in a cell. Several research groups have lysed cells with physical and chemical methods.[11] Common physical methods for implementation of cell lysis involve mechanical force or an electric field. Li and Harrison[12] controlled the flow of the cell solution using electro-osmosis while simultaneously injecting a sodium dodecyl sulfate (SDS) solution for cell lysis. After lysis, the released cellular materials were recovered using an electric field. Wang and Lu[13] designed microfluidic channels with geometric variation to lyse cells by intensifying the electric field at narrow sections of the microchannels. Their results showed that at higher electric field, cells lysis took only a few milliseconds. Sasuga et al.[14] manufactured microporous structures from micro arrays to capture cells before performing cell lysis using CelLytic-M. Vulto et al.[15] designed a microchip for cell lysis and RNA purification; as the cell was lysed, RNA was extracted using gel electrophoresis. The experiment showed that after cell lysis, short fragments of RNA were obtained immediately without removing impurities. Terao et al.[16] fabricated microstructures that captured yeast cells while lysing the yeast cells with a lysis solution and stretching DNA. Hung and Chen[17] integrated atomic force microscope (AFM) and electro-osmosis and used the AFM's tip to lyse human cells that were immobilized to the glass surface and stretch DNA.

Most previous studies have demonstrated cell separation, collection and cell lysis using animal or human samples (e.g. blood, tissue biopsies, etc.). Few studies have used microchips or microdevices to conduct plant analysis; for example, root-developing effects[18] or pollen tube growth.[19] Therefore, this study develops a microfluidic device to demonstrate the rapid collection and lysis of plant cells from plant leaves.

One difference between a plant cell and an animal cell is that plant cells have a cell wall composed primarily of cellulose. This wall maintains the outer shape of the cell. Thus, to extract substances from the plant cell, the cell wall must be removed. Plant cells with their cell wall removed are called protoplasts. The traditional method for extracting protoplasts includes enzymatic lysis of the cell wall, filtration of impurities and protoplast collection after centrifugation.

This study uses microfabrication combined with trace drugs to develop a microfluidics device that can isolate, collect and lyse orchid protoplasts. Protoplasts are isolated using an enzymatic solution and filtered by designed microsieves on the U-bends of the main flow channel to collect protoplasts. The protoplasts are lysed with a SDS solution to release DNA. We demonstrate real-time protoplasts collection and lysis in the microfluidic device. This platform can be applied to rapid DNA analysis and viruses detection in plant cells.

Materials and methods

The microfluidic device design is shown in Figure 1(a). In this study, the microsieves in the U-bend of the main flow channel have two designs: a concave sieving array and a convex–concave sieving array. The concave sieving array design has a protoplast sieving array (with a square length of 25 μm) covering the concave surface of the U-bend (on the left side of Figure 1(b)). For the convex–concave sieving array, the protoplast sieving array (with a square length of 50 μm) is placed on the convex surface at the entrance of the U-bend and on the concave surface where fluid exits the U-bend (shown on the right side of Figure 1(b)). The widths of the main flow channel and the protoplast-collecting channels are 600 μm and 300 μm, respectively. The distance between the microsieves is 10 μm. In addition, Figure 1(c) shows a rectangular microstructure (with a square length of 60 μm) designed as a nucleic acid analysis zone. Because the microsieves in the U-bends have 10- μm gaps, only protoplasts can pass through; thus, the impurities (larger than 10 μm) remain in the main flow channel.

This study used negative photoresist SU8-2025 and polydimethylsiloxane (PDMS) to fabricate microfluidics for protoplasts collection and lysis. A glass was spin coated with negative photoresist and then soft baked, post-exposure baked and developed, and washed with isopropyl alcohol (IPA) and deionized (D.I.) water. The microchannels fabricated from SU8-2025 were approximately 60 μm thick. The fabricated negative photoresist structure was cast with PDMS mixture (Sylgard 184 A:B = 10:1, Dow Corning) and heated for PDMS thermal curing (100 °C for 1 h).[20] After the PDMS mould was stripped, PDMS surface modification was conducted with oxygen plasma to enable bonding with a glass. The fabricated PDMS microfluidic device is shown in Figure 2(a). The experimental system set-up is shown in Figure 2(b). The microfluidic device was placed on the inverted fluorescent microscope platform (IX71, Olympus, Japan) and the flow of solution in it was driven with a peristaltic

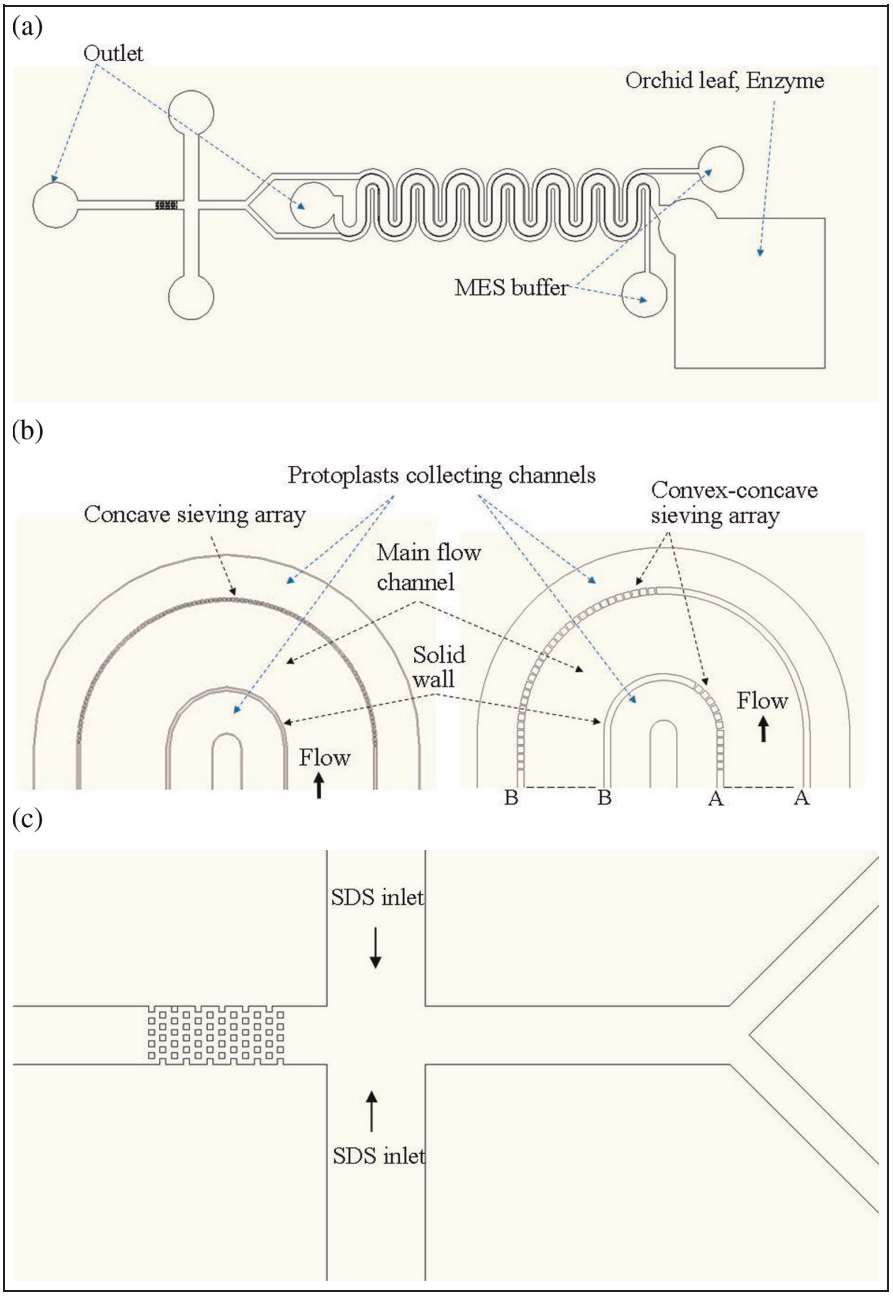

Figure 1. Schematic diagram of orchid protoplasts collection and lysis microfluidic device: (a) the microfluidic device; (b) concave sieving array (left side) and convex–concave sieving array (right side). The dotted lines of A-A and B-B indicate the entrance and the exit of the U-bend respectively. (c) Enlarged view of protoplasts lysis zone.

pump (ISMATEC, 11446), which was arranged downstream of the chip and interfaced with thin soft tube.

The orchid samples used for this experiment were *Phalaenopsis Chiada Pioneer* (kindly supply from the Horticultural Technology Center in National Chiayi University). We obtained a suitable portion of a *Phalaenopsis* leaf. The leaf surface was cleaned with 70% ethanol for sterilization and put in the inlet of the microfluidic device. The cell wall was degraded by injecting enzyme solution and the protoplasts were obtained; meanwhile, the nucleic acid dye 4'-6-diamidino-2-phenylindole (DAPI) was added to observe fluorescence of the protoplasts.

To analyze the protoplast collection efficiency, we used software (COMSOL Multiphysics 3.3) to simulate the flow field of the main flow channel. The following conditions and governing equation were assumed and applied: incompressible three-dimensions for the Navier–Stokes equation, zero as the inlet pressure for the initial condition, 1 μl/min and 5 μl/min for the flow rates and no-slip for the boundary condition.

$$\nabla \cdot \boldsymbol{V} = 0 \tag{1}$$

$$\rho\left(\frac{\partial \boldsymbol{V}}{\partial t} + \boldsymbol{V} \cdot \nabla \boldsymbol{V}\right) = -\nabla p + \rho \boldsymbol{g} + \mu \nabla^2 \boldsymbol{V} \tag{2}$$

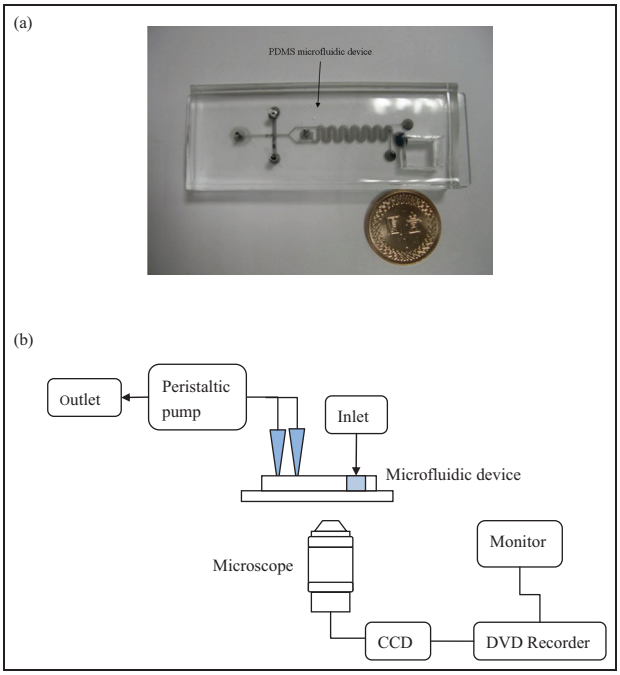

Figure 2. (a) Photograph of polydimethylsiloxane (PDMS) microfluidic device; (b) schematic diagram of experimental system set-up.

In the equations, p is the pressure, ρ is the density of the fluid, μ represents the absolute viscosity, $\boldsymbol{V}$ signifies the vector of flow velocity, t is the time, and finally $\boldsymbol{g}$ is the vector of gravity acceleration (see notation list in Appendix 1).

Experimental procedure: feed 0.15 g of leaves cut into lengths of 1–2 mm into the inlet of microfluidic device, add 400 µl of enzyme solution (10 mM 2-(N-Morpholino) ethanesulfonic acid (MES), 0.6 M mannitol, 1 mM $CaCl_2$, 0.75% macerozyme, 1.5% cellulase, 0.1% bovine serum albumin (BSA), 5 mM β-mercaptoethanol), and inject isotonic MES buffer solution (pH5.7, 4 mM MES) into both protoplasts collecting channels at room temperature. As the solution flows towards the outlets by using the peristaltic pump, the wall-free protoplasts are filtered using a sieving array, and enter the collecting channels. The protoplasts flow to the confluence of the collecting channels and are guided into the lysis zone. After protoplast lysis, DNA is released into the solution, which flows towards the rectangular microstructures.

3. Results and discussion

To compare the protoplast collection speed between the traditional method and that proposed in this study, we collected protoplasts using the traditional method in steps as listed below.

1. Plant leaves were obtained and wiped with 70% ethanol.
2. Leaves were cut into lengths of approximately 1 mm and placed in a culture dish before adding an enzymatic solution.

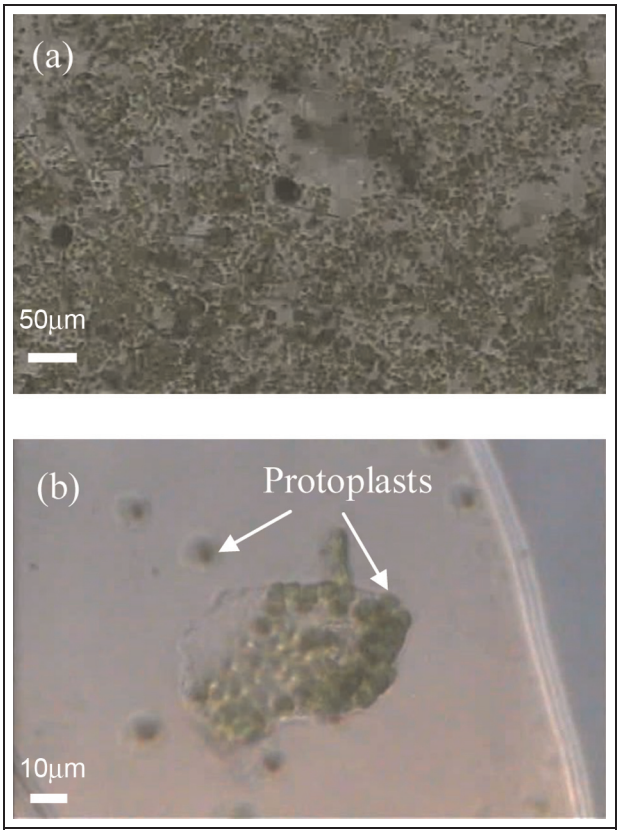

Figure 3. Photographs of separated protoplasts: (a) protoplasts in culture dish; (b) enlarged view of protoplasts.

3. The mixture was placed under a vacuum for 30 min.
4. The mixture was incubated at room temperature for 2 h; after every 10 min of incubation, the dish was shaken.
5. Filtration was carried out using a 70 µm nylon cell filter and centrifuge.
6. The supernatant was removed and the protoplasts were suspended in buffer solution, centrifuged again; the washing process was repeated three times.
7. Finally, the protoplasts were put in suspension using 0.5 ml of buffer solution.

The protoplast extraction experiment took approximately 4 h to complete, and the results are shown in Figure 3. These results reveal that a large amount of chloroplasts was observed in the extracted solution because of the disrupted protoplasts. Some non-degraded cell walls and other impurities were also present. Additionally, a small amount of intact protoplasts were extracted.

In this study, a microfluidic device is developed for collecting protoplasts. By placing the microfluidic device on the microscope platform, connecting the peristalsis pump at the exit, and placing the leaves, enzyme solution and buffer at the inlet, protoplasts were observed in the main channel after approximately 20 min. The protoplasts flowed toward the concave sieving array of the main flow channel at a rate of 5 µl/

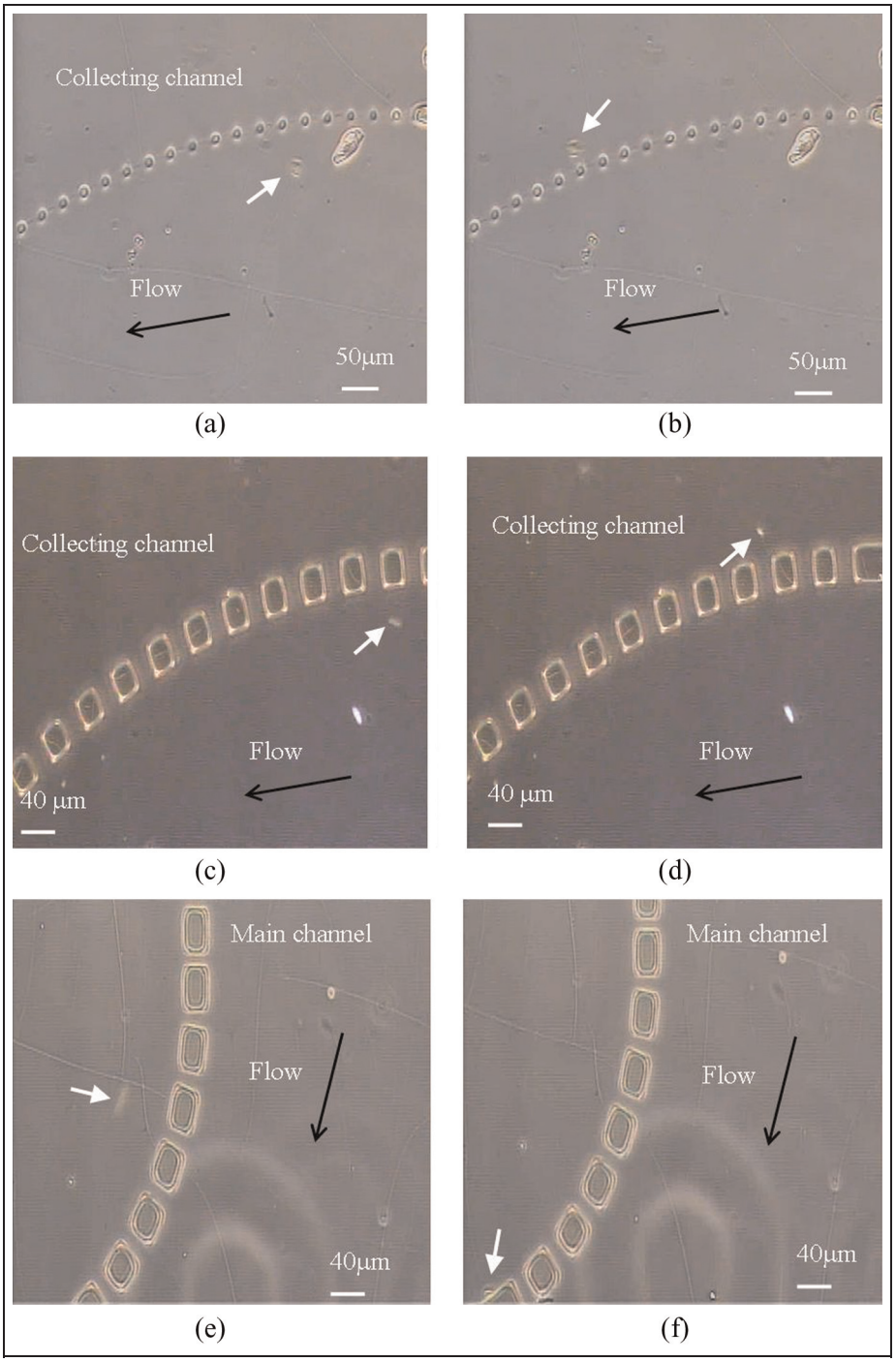

Figure 4. Photographs of protoplast collection using concave sieving array ((a) and (b)) and convex–concave sieving array ((c) to (f)). In the figure, protoplasts are in the main flow channel ((a) and (c)) and flow into the collecting channel ((b) and (d)) at the U-bend. For the convex–concave sieving array, it is observed that the protoplasts in the collecting channel (e) will not flow back to the main flow channel (f).

min, as shown in Figure 4(a) and (b) (indicated by a white arrowhead). Meanwhile, we found that some protoplasts in the outer collecting channel flowed back into the main channel through the sieving array when the solution passed the entrance to the U-bends (data not shown).

Figure 4(c) to (f) shows the results of protoplast collection using a convex–concave sieving array in the U-bends of the microfluidic device. The protoplast flows through the microsieves on the concave surface and into the collecting channel (indicated by a white arrowhead in Figure 4(c) and (d)). At the U-bends' entrance, the protoplasts sieving array is placed on the convex surface to allow the protoplasts to flow into the inner collecting channels (data not shown). The protoplasts sieving array is designed on the concave surface, whereas the solid wall is designed on the convex surface as fluid exits each bend. This enables the protoplasts to

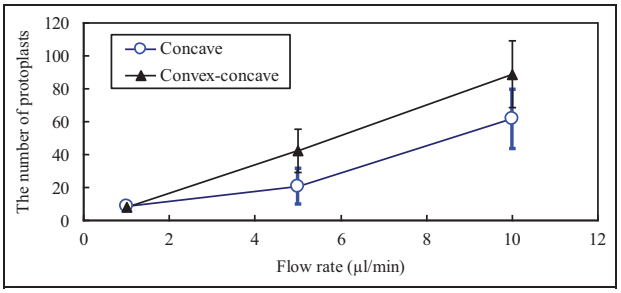

Figure 5. The amount of protoplasts at various flow rates collected at the confluence of the collection channels for the concave sieving array and the convex–concave sieving array (for 10 s).

flow into the outer collecting channel; protoplasts collected in the inner collecting channel will not flow back to the main flow channel (indicated by a white arrowhead in Figure 4(e) and (f)).

To compare the protoplast collecting efficiency between the concave sieving array and the convex–concave sieving array, the protoplast amounts at various flow rates were collected (for 10 s) at the confluence of the collecting channels. The number of times the protoplasts calculation was carried out for both two microsieves designs was nine on different days. The observation and collection results are shown in Figure 5. The result indicates that the number of protoplasts collected increases at higher flow rates, regardless of the variation in sieving array. At a flow rate of $\geqslant 5\,\mu$l/min, the protoplast collecting efficiency of the convex–concave sieving array is superior to that of the concave sieving array. This is because the number of protoplasts in the collecting channel increased and did not flow back into the main flow channel at higher flow rates.

To analyze the flow characteristics of the U-bends, the software was used to simulate the flow in the main flow channel. Figure 6 shows the velocity distribution of varied flow rates at half the channel height. These results reveal that within the flow field, the velocity distribution has a similar trend regardless of varied flow rates. At the U-bends' entrance, the flow velocity is increased on the convex surface and the velocity vectors arrows are towards the convex surface. At the U-bends' exit, the velocity vectors shift toward the concave surface and move away from the convex surface. The simulated results for the flow at the U-bend also indicate that the convex–concave sieving array can prevent back-flowing of filtrate from the collecting channels into the main flow channel as the fluid path curves along the U-bend. Therefore, the design of a convex–concave sieving array enhances its protoplast collecting efficiency compared to that of the concave sieving array. In addition, the time for protoplast collection in this study was reduced to approximately 0.5 h.

The protoplasts lysis results by using microfluidics with convex–concave sieving array are shown in Figure 7. The protoplasts in both collecting channels flow

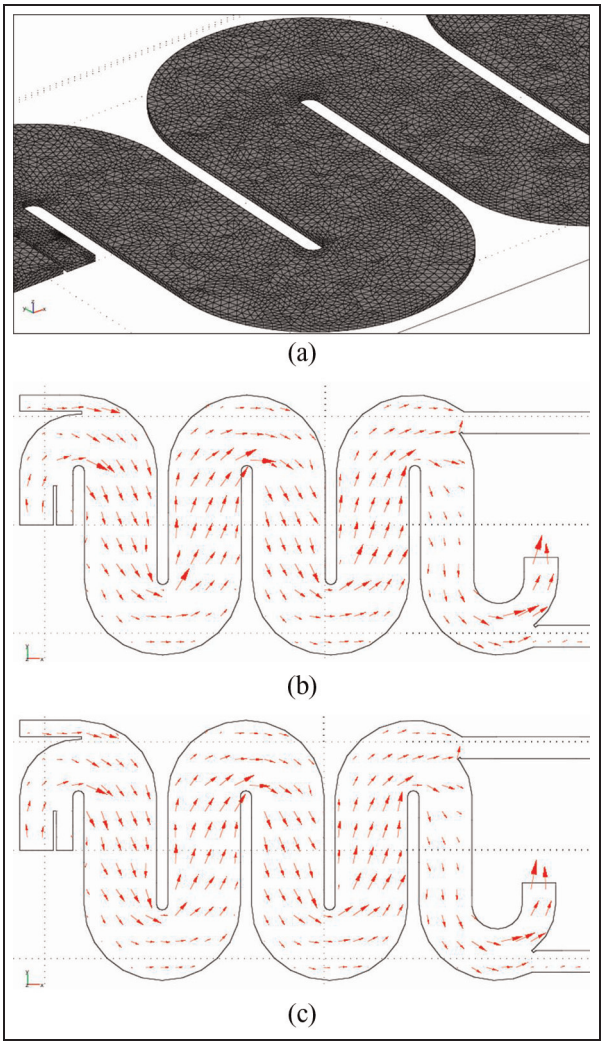

Figure 6. The simulated results for the flow at the U-bend: (a) mesh generation for computation; (b) at a flow rate of 1 μl/min; (c) at a flow rate of 5 μl/min (arrows indicate the velocity vectors).

towards the confluence and the lysis zone. The lysis solution of 1% SDS was injected into the lysis zone from two inlets (indicated by two white arrowheads in Figure 7(a) and (b)). The two injecting SDS solutions are to focus the protoplasts stream and to sheath a core stream in the microchannel (Figure 7(a) and (b)), as stated by Simonnet and Groisman.[21] In Figure 7, the protoplasts lysis and DNA release is observed using fluorescence. Because neither of the two injecting SDS solutions contains DNA, only the DNA fluorescence in the core stream is observed, as shown in Figure 7(b). The DNA flow in the center is focused to a single stream and extended to the downstream of the channel, as shown in Figure 7(c) (flow rate of 5 μl/min) and (e) (flow rate of 1 μl/min). The extending DNA stream makes contact with rectangular microstructures in microchannels (Figure 7(d) and (f)). Meanwhile, comparing the fluorescence intensity of the focused stream between the lower and higher flow rates, the fluorescence intensity of DNA at the higher flow rate of 5 μl/min is increased (Figure 7(c) and (d)). This result indicates

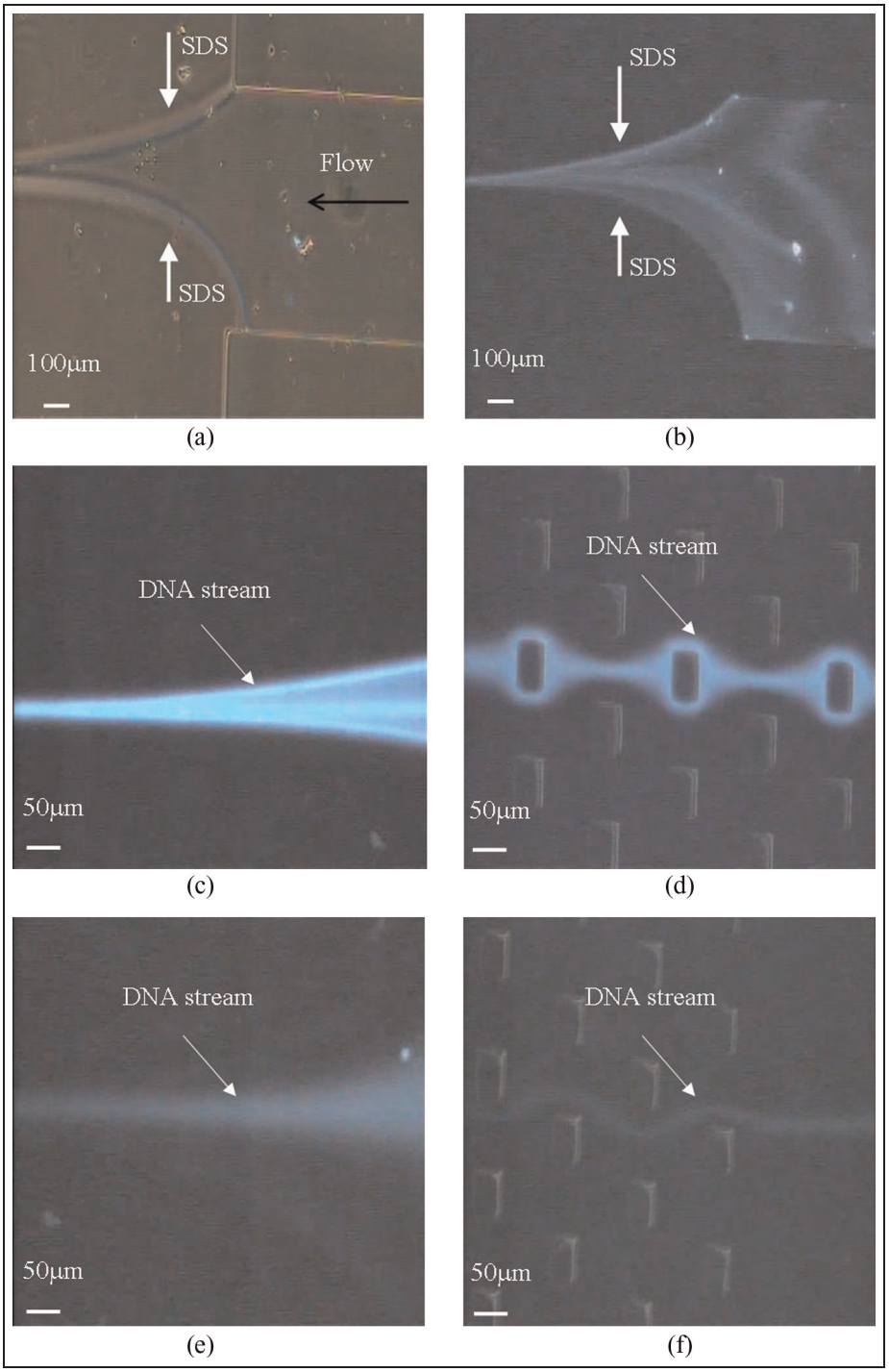

Figure 7. Photographs of protoplasts lysis and DNA release: (a) the bright field view of sheath flow; (b) the fluorescence view of protoplasts lysis; (c) extending DNA stream at 5 μl/min; (d) DNA stream making contact with microstructures at 5 μl/min; (e) extending DNA stream at 1 μl/min; (f) DNA stream making contact with microstructures at 1 μl/min.

that the amount of DNA content within the stream is larger, which suggests that the protoplasts lysis process is more effective at a high flow rate than at a low flow rate.

4. Conclusions

This study has developed a microfluidics device that is capable of the real-time isolation, collection and lysis of protoplasts from plant leaves. To achieve rapid protoplasts collection, the microsieves in the PDMS microfluidics device were used to isolate the protoplasts. The procedure of protoplasts collection and lysis was integrated with an image process system for real-time observation. When injecting enzyme solution, the microfluidics device successfully isolated and collected protoplasts from *Phalaenopsis* leaves. To compare the efficiency of protoplast collection, the flow simulation

result of the U-bend was used to analyze the arrangement of microsieves in the main flow channel. The experiment and simulation results indicate that the protoplast collecting efficiency is higher for the convex–concave sieving array when compared with the concave sieving array at a flow rate of $\geqslant 5\,\mu$l/min. In addition, we reduced the protoplast collection time in this study to approximately 0.5 h, compared to the 4 h required by the traditional method. After the injection of 1% SDS lysis solution at a higher flow rate of $5\,\mu$l/min, protoplasts were rapidly lysed within the microchannels and released DNA into the solution. The flow of lysed protoplasts focuses to a single stream by sheath flow and makes contact with microstructures in the microchannels. These results suggest that rapid plant protoplast collection and lysis can be applied to accelerate the detection of plant DNA or RNA. In future work, we will immobilize a fluorescent labeled nucleic acid probe on the rectangular microstructures in the microfluidic device. This would then be used to detect viruses rapidly in plant cells or for plant DNA analysis.

Acknowledgements

This work was supported by NSC, Taiwan (grant number NSC 99-2313-B-415-008-MY2). We thank Professor Shan-Te Hsu at National Chiayi University for the supply of *Phalaenopsis*.

References

1. Reyes DR, Iossifidis D, Auroux PA, et al. Micro total analysis systems. 1. Introduction, theory, and technology. *Anal Chem* 2002; 74: 2623–2636.
2. Auroux PA, Iossifidis D, Reyes DR, et al. Micro total analysis systems. 2. Analytical standard operations and applications. *Anal Chem* 2002; 74: 2637–2652.
3. Kovarik ML, Gach PC, Ornoff DM, et al. Micro total analysis systems for cell biology and biochemical assays. *Anal Chem* 2012; 84: 516–540.
4. Tsutsui H and Ho CM. Cell separation by non-inertial force fields in microfluidic systems. *Mech Res Commun* 2009; 36: 92–103.
5. Kuo JS, Zhao Y, Schiro PG, et al. Deformability considerations in filtration of biological cells. *Lab Chip* 2010; 10: 837–842.
6. Washizu M. Biological applications of electrostatic surface field effects. *J Electrostat* 2005; 63: 795–802.
7. Shafiee H, Sano MB, Henslee EA, et al. Selective isolation of live/dead cells using contactless dielectrophoresis (cDEP). *Lab Chip* 2010; 10: 438–445.
8. Grier DG. A revolution in optical manipulation. *Nature* 2003; 424: 810–816.
9. Pamme N. Magnetism and microfluidics. *Lab Chip* 2006; 6: 24–38.
10. Lien KY, Chuang YH, Hung LY, et al. Rapid isolation and detection of cancer cells by utilizing integrated microfluidic systems. *Lab Chip* 2010; 10: 2875–2886.
11. Hung MS and Chang YT. Single cell lysis and DNA extending using electroporation microfluidic device. *Biochip J* 2012; 6: 84–90.
12. Li CH and Harrison DJ. Transport, manipulation, and reaction of biological cells on-chip using electrokinetic effects. *Anal Chem* 1997; 69: 1564–1568.
13. Wang HY and Lu C. Electroporation of mammalian cells in a microfluidic channel with geometric variation. *Anal Chem* 2006; 78: 5158–5164.
14. Sasuga Y, Iwasawa T, Terada K, et al. Single-cell chemical lysis method for analyses of intracellular molecules using an array of picoliter-scale microwells. *Anal Chem* 2008; 80: 9141–9149.
15. Vulto P, Dame G, Maier U, et al. A microfluidic approach for high efficiency extraction of low molecular weight RNA. *Lab Chip* 2010; 10: 610–616.
16. Terao K, Kabata H and Washizu M. Extending chromosomal DNA in microstructures using electroosmotic flow. *J Phys Condens Matter* 2006; 18: S653–S663.
17. Hung MS and Chen PC. Extending DNA from a single cell using integrated system of electro-osmosis and AFM. *J Med Biol Eng* 2010; 30: 29–34.
18. Meier M, Lucchetta EM and Ismagilov RF. Chemical stimulation of the *Arabidopsis thaliana* root using multilaminar flow on a microfluidic chip. *Lab Chip* 2010; 10: 2147–2153.
19. Yetisen AK, Jiang L, Cooper JR, et al. A microsystem-based assay for studying pollen tube guidance in plant reproduction. *J Micromech Microeng* 2011; 21: 054018.
20. Duffy DC, McDonald JC, Schueller OJA, et al. Rapid prototyping of microfluidic systems in poly(dimethylsiloxane). *Anal Chem* 1998; 70: 4974–4984.
21. Simonnet C and Groisman A. Two-dimensional hydrodynamic focusing in a simple microfluidic device. *Appl Phys Lett* 2005; 87: 114104.

Appendix 1

Notation

$\boldsymbol{g}$	gravity acceleration (m/s^2)
p	pressure (N/m^2)
t	time (s)
$\boldsymbol{V}$	flow velocity (m/s)
μ	absolute viscosity (N s/m^2)
ρ	density of fluid (kg/m^3)
∇	del vector operator